Photoelectron Imaging on Time-Dependent Molecular Alignment Created by a Femtosecond Laser Pulse

Masaaki Tsubouchi,[1,2] Benjamin J. Whitaker,[2,*] Li Wang,[2,†] Hiroshi Kohguchi,[1,2] and Toshinori Suzuki[1,2,3,‡]

[1]*Graduate University for Advanced Studies, Myodaiji, Okazaki 444-8585, Japan*

[2]*Institute for Molecular Science, Myodaiji, Okazaki 444-8585, Japan*

[3]*PRESTO, Japan Science and Technology Corporation, Kawaguchi 332-0012, Japan*

(Received 26 December 2000)

Rotational wave packet revivals on an excited electronic state have been measured by femtosecond time-resolved photoelectron imaging for the first time. The first full revival at 82 ps of S_1 (n, π^*) pyrazine was clearly observed in the time dependencies of the photoelectron intensity and the photoelectron angular distribution (PAD). The PAD, measured for laser aligned pyrazine, clearly reflects the different characters of π^* and $3s$ molecular orbitals.

DOI: 10.1103/PhysRevLett.86.4500 PACS numbers: 33.60.–q

Coherent excitation of an ensemble of rotational states in a given vibronic band creates a rotational wave packet that revives at rotational periods of a molecule [1]. Felker and Zewail observed these revivals by laser-induced fluorescence to determine the rotational level structures of large molecules that are difficult to study in the frequency domain [2–4]. The method is known as rotational coherence spectroscopy (RCS).

Superior time resolution and the possibility to apply RCS to weakly or nonfluorescent molecules can be obtained, in principle, by a pump-probe ionization scheme. Scherer *et al.* [5] demonstrated this approach more than a decade ago, although only a few examples have been reported thus far [6,7]. Note that the method of monitoring the total ion current is problematic in that ionization to various cationic vibronic levels with different transition dipole moment directions are mixed together, which significantly reduces the rotational revival signature in the total ion current (total cross section). In addition, many large molecules undergo electronic dephasing after photoexcitation. Ionization can occur both from the optically prepared (bright) state or the background (dark) states involved in electronic dephasing. It is quite interesting to observe rotational revivals in the dark manifold, but this is not possible with pump-probe mass spectrometry for the same reason.

One of the objectives of this work is to present RCS in the form of time-resolved photoelectron imaging (PEI) that discriminates and visualizes the revivals in the optically bright and dark states in an electronic dephasing process. The rotational revivals are detected not only in the energy-selected photoelectron intensity (partial cross section) but also in the photoelectron angular distribution (PAD), i.e., the differential cross section.

The other objective is to demonstrate a new way to approach the PAD measured for a molecule fixed in space that has for some time been an experimental goal in photoionization dynamics. Such measurements have previously been achieved by coincidence detection of daughter ions and electrons in dissociative ionization [8–10]. However, the requirement of prompt dissociation of the ion restricts the method to small molecules dissociated with relatively high energy photons. An alternative approach is to measure the PAD for an ensemble of aligned [11–14] or oriented [15] molecules. McKoy [11,12], Zare [13,14], and co-workers studied photoionization of laser-aligned NO molecules with nanosecond lasers. Similar experiments with ultrafast lasers will be quite interesting [16–18], since, with short pulses, the laser field can be easily increased to achieve much stronger alignment. Here, we demonstrate the PAD measurement for maximally aligned molecules in the weak field limit, $F(\theta) = \cos^2\theta$, from which extension to the stronger laser field will be straightforward.

The experimental setup used is essentially identical to that described in our previous PEI studies [19,20]. However, two key modifications were made to improve the stability of the system and the efficiency of data acquisition. These are the use of a 1 kHz Nd:YLF-pumped Ti:sapphire regenerative amplifier instead of a Nd:YAG-pumped 10 Hz system, and a continuous molecular beam replacing a pulsed beam. Briefly, the 82 MHz, 300 mW output of a diode-pumped Ti:sapphire laser was amplified by a Nd:YLF-pumped regenerative amplifier to generate a 1 kHz pulse train of $\sim$2.5 mJ pulse^{-1} light centered at $\sim$802 nm. This light was split into two equal intensity beams, one of which pumped an optical parametric amplifier to generate tunable UV pump light ($\sim$324 nm) in resonance with the 0_0^0 band of the $S_1\ ^1B_{3u}(n, \pi^*) \leftarrow S_0\ ^1A_g$ transition of pyrazine. The other beam was frequency doubled to $\sim$401 nm in a thin β-BaB_2O_4 crystal to produce the probe light. The cross correlation was ca. 200 fs. The probe beam was optically delayed with respect to the pump beam using a hollow corner cube on a computer-controlled delay stage. Then, the two beams were merged by a dichroic mirror and directed into the molecular beam chamber. The laser intensities at the molecular beam were estimated to be 8×10^{10} and 4×10^{10} W/cm^2. In some of the experiments described in the present paper, we also employed 200 nm probe light generated by nonlinear mixing of the fundamental

 0031-9007/01/86(20)/4500(4)$15.00

and third harmonic of Ti:sapphire laser output. Pyrazine, 2% seeded in molecular nitrogen at a stagnation pressure of ~500 Torr, was expanded from a pinhole 50 μm in diameter to generate a continuous molecular beam. The beam was skimmed and introduced into the ionization chamber where the background pressure (beam on) was ca. 10^{-7} Torr. The effective rotational temperature of pyrazine was determined to be 20 K from an analysis of the rotational contour of the $S_1 \leftarrow S_0$ 0_0^0 band recorded using a nanosecond dye laser.

Figure 1 shows the molecular structure and an energy level diagram of pyrazine. The pump pulse excited pyrazine to the S_1 0^0 level, and the subsequent 401 nm probe pulse ionized this level by a two-photon process. The generated photoelectrons were accelerated in an electric field parallel to the molecular beam and detected by a position sensitive imaging detector. Two-dimensional space focusing was employed to make an image sensitive only to the linear momentum of the photoelectrons parallel to the face of the detector and not the spatial position of ionization [21]. The field-free region of the electron flight path was shielded against stray magnetic fields by a μ-metal tube. The imaging detector consisted of a 40 mm diameter dual microchannel plate assembly coupled to a phosphor screen that was viewed through a fiber bundle by an intensified video-rate charge-coupled-device (CCD) camera. The video signal from the camera was recorded on a personal computer.

Although the number of photoelectrons created by each laser shot was small, a slow frame rate (25 Hz) camera integrated the data for 40 laser shots per frame. Thus, the light spots due to different electrons hitting the detector overlap each other in a single frame, which hampered centroiding or thresholding calculations [22–24]. However, the quality of the photoelectron images was sufficiently high.

Figure 2(a) shows a typical photoelectron image measured at a time delay of 30 ps between the pump (324 nm) and probe (401 nm) pulses. The image is an inverse Abel transform of the observed data, representing a section of the 3D photoelectron scattering distribution. The pump and probe laser polarization are both vertical in the figure. The observed image consists of three major rings with different radii corresponding to the photoelectron kinetic energies of 37, 101, and 643 meV. The sharp ring structure indicates that all of these ionization processes occur with the vibrational selection rule $\Delta v = 0$ via intermediate Rydberg states at the energy of $\omega_1 + \omega_2$. Strong anisotropy in the photoelectron image also points to atomiclike electron orbitals in the intermediate states. From comparison with the literature [25], the Rydberg states contributing to the two outer rings were assigned to the $3s$ (^1A_g) and $3p$ ($^1B_{3u}$ or $^1B_{2u}$) Rydberg states. This refutes our earlier speculation [19] that the middle peak might be due to ionization of the T_2 (π, π^*) state. The time dependencies of photoelectron intensity for the three rings are shown in Fig. 2(b). The two outer

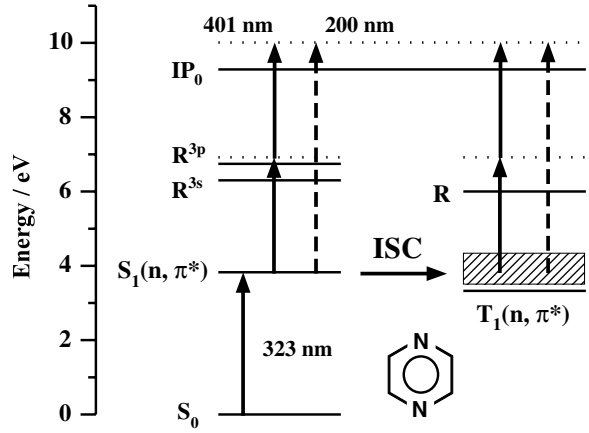

FIG. 1. Molecular structure and schematic energy diagram of pyrazine.

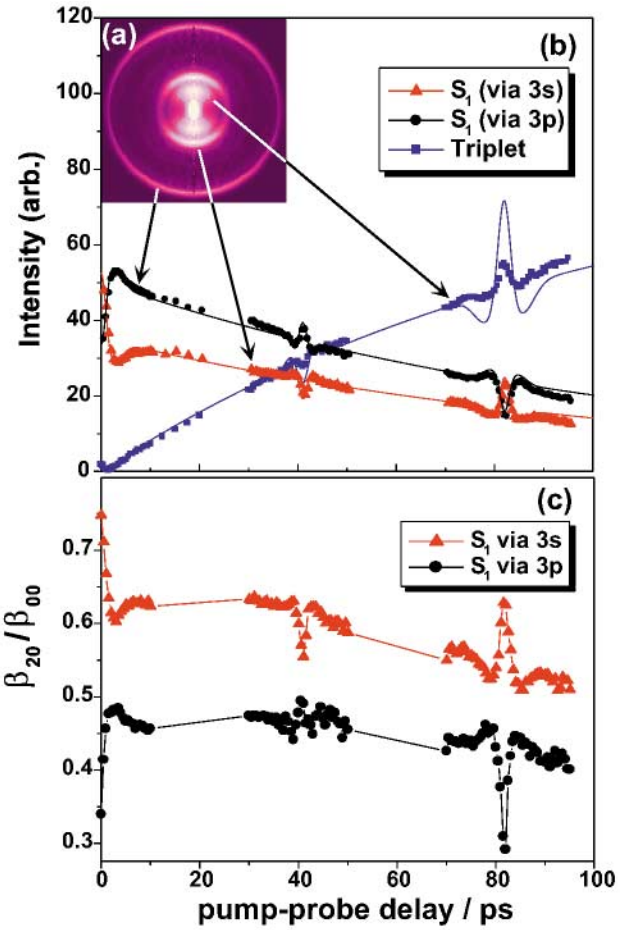

FIG. 2 (color). (a) Inverse Abel transformed photoelectron image of the [1 + 2′] PEI of pyrazine via the S_1 $B_{3u}(n, \pi^*)$ 0^0 level observed at the time delay of 30 ps. The original image was integrated for 80 000 laser shots. (b) Time evolution of three major components in the [1 + 2′] PEI. Circle (○), triangle (△), and square (□) represent the angle-integrated intensity for the outer (KE = 643 meV), middle (101 meV), and inner ring (37 meV), respectively. Solid lines are a simulation taking into account the rotational coherence. (c) β_{20}/β_{00} as a function of pump-probe time delay in the [1 + 2′] PEI.

distributions decay as a function of time ($\tau = 110$ ps), while the inner one grows with the same time constant, corresponding to the intersystem crossing from the S_1 to the triplet manifold, as assigned in our previous work [19,20]. More importantly, all of these curves exhibit periodic revival structures. Note, in particular, that the rotational revival appears in the photoelectron signal from the triplet manifold.

We have analyzed these revival features based on the theory of RCS reported by Felker and Zewail [3]. For simplicity, we approximated the S_1 state of pyrazine as an oblate symmetric top (the A,B, and C rotational constants are 6.1035, 6.0813, and 3.0477 GHz, respectively, [25]). From other experiments, we can fix the rotational temperature, 20 K, of our sample and the intersystem crossing rate of S_1 to the triplet manifold, 9.1×10^9 s^{-1}. By assuming the transitions from S_1 to R_n^{3s} and to R_n^{3p} to be parallel and perpendicular, respectively, simulation of the RCS revivals agrees almost perfectly with observation, as shown in Fig. 2(b). The transition from the S_1 ($^1B_{3u}$) to the $3p$ ($^1B_{3u}$ or $^1B_{2u}$) state is vibronically induced by excitation of the mode 11 (b_{3u}), making the transition a perpendicular type. The revivals in the triplet manifold were treated phenomenologically by assuming that the electronic dephasing occurs exponentially. The rotational constants known for the T_1 0^0 level [26] were assumed for the triplet manifold. The peaks observed for the triplet state are, however, much weaker than the simulation. Note that the number of triplet levels coupled to S_1 is estimated to be 20 [27], so it is likely that slightly different rotational constants among these highly excited triplet vibronic levels diminish the revival peaks.

Figure 3 shows the time dependence of the PAD following ionization of the S_1 state via the $3p$ Rydberg state. Photoelectron images were recorded at pump-probe delay intervals of 500 fs around the positions of the first full revival of the rotational wave packet at 82 ps. At the full revival, the PAD exhibits a small enhancement in the direction of 90°. More quantitatively, the PAD measured at each time delay was fit to the following form [28]:

$$I(\theta) = \beta_{00}Y_{00}(\theta,\phi) + \beta_{20}Y_{20}(\theta,\phi) + \beta_{40}Y_{40}(\theta,\phi) + \beta_{60}Y_{60}(\theta,\phi), \quad (1)$$

where Y_{LM} are spherical harmonics. We found β_{60} to be negligible. The ratio β_{20}/β_{00} thus obtained for ionization of S_1 via the $3s$ and $3p$ Rydberg states also clearly shows the rotational revivals [Fig. 2(c)].

In the present case, the pump pulse creates a time-dependent alignment $A_{20}(t)$ in the S_1 state, and the probe pulse transfers this alignment to rotational levels in the Rydberg states. Since these states are ionized instantaneously within a probe laser pulse, the PAD is modulated only by the time dependence of $A_{20}(t)$ in the S_1 state.

The experimentally determined time-dependent PAD opens a way to access the PAD in the molecular frame. This is not a novel observation, but previous measurements of time-dependent PADs have proven very difficult to interpret because of complications arising from concomitant vibrational and rotational dynamics [18]. By contrast, in pyrazine, as measured by PEI, the rotational coherence effects on the PADs are very clear. At time $t = 0$, the system maximally aligns the transition dipole moment to the pump laser polarization with a $\cos^2\theta$ distribution (one-photon absorption case). Specifically, the alignment is created by a parallel transition from S_0, so the principal axis of the molecule is aligned predominantly parallel to the pump laser polarization. Figure 4(a) shows a polar plot of the PAD recorded by [1 + 1′] ionization measured with probe light at 200 nm aligned parallel to the pump laser polarization. The PAD at $t = 0$ shows a characteristic fourfold distribution that clearly indicates the photoelectrons are ejected not only along the probe laser polarization (out of the molecular plane) but also perpendicular to it (in the plane). At 2.8 ps after the pump pulse, the alignment parameter for pyrazine at the rotational temperature of 20 K almost vanishes, so the ensemble of molecules is randomly oriented in space. At this time, the characteristic fourfold feature also completely vanishes.

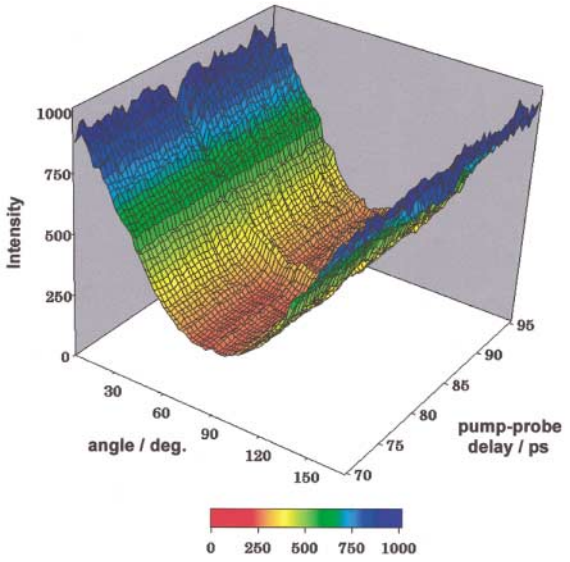

FIG. 3 (color). Time dependence of photoelectron angular distribution obtained for [1 + 2′] PEI via S_1 0^0 and $3p$ 11^1 Rydberg states. Pump-probe delay was scanned from 70 to 95 ps with 500 fs intervals. The first full revival of the rotational wave packet is at 82 ps in agreement with theory.

It is interesting to compare the PAD for ionization from different orbitals. The PAD observed by two-photon ionization of S_1 via $3s$ is interpreted as the PAD resulting from one-photon ionization of the $3s$ state aligned by $\omega_1 + \omega_2$ two-step excitation from the S_0 state. The PAD measured for the $3s$ state shown in Fig. 4(b) is dramatically different from that in Fig. 4(a). At time delay $t = 0$ between the pump ($S_1 \leftarrow S_0$) and probe laser pulses (ion $\leftarrow 3s \leftarrow S_1$), the principal axis of pyrazine in the $3s$ state is maximally aligned with a $\cos^4\theta$ distribution with respect to the laser

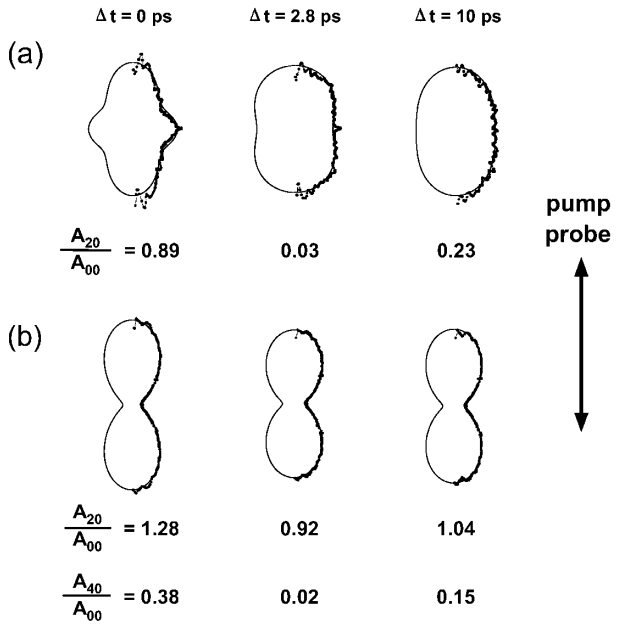

FIG. 4. Polar plots of the PAD observed for one-photon ionization of laser-aligned pyrazine in the (a) S_1 0^0 and (b) $3s$ Rydberg states. The pump-probe time delays and the alignment parameters are shown in the figure. Solid lines are theoretical fits.

polarization. The corresponding PAD shows almost a $\cos^2\theta$ distribution with respect to the probe laser polarization, indicating that photoelectron ejection in the plane of pyrazine is minimal. The time dependence of the PAD is also rather weak. This is because the probe laser pulse aligns and ionizes the $3s$ state within the pulse duration so that the alignment of the $3s$ Rydberg state of pyrazine is always stronger than $\cos^2\theta$.

Both the S_1 and $3s$ states have a hole in the $n^+(a_g)$ orbital, and the outer electrons occupy $\pi^*(b_{3u})$ and $3s(a_g)$ orbitals, respectively. The difference in the PAD observed for these two cases of ionization near the threshold can be ascribed to the different characters of the one-electron molecular orbitals. The $3s$ orbital is atomiclike and produces a predominant $p\pi$ outgoing wave in ionization, although the fact that β_{20}/β_{00} is smaller than its limiting value $(2/\sqrt{5})$ is indicative of the deviation of the electron-core potential from radial symmetry. In contrast, the parallel transition out of the $\pi^*(b_{3u})$ orbital requires outgoing partial waves of a_g symmetry. The result suggests that this a_g wave has σ (or n) component presumably along the z axis through the N atoms.

In conclusion, we have demonstrated the use of time-resolved photoelectron angular distributions for observing rotational revivals in the excited states. The PADs measured for a laser-aligned molecule showed clear signatures of the different symmetry properties of the molecular orbitals. A higher pump intensity will provide stronger alignment and a further structured PAD is anticipated for ionization of the π^* electron. Photoelectron imaging in conjunction with an intense laser field is in progress in our laboratory.

*On leave from School of Chemistry, University of Leeds, Leeds LS2 9JT, United Kingdom.
†Permanent address: Dalian Institute of Chemical Physics, Dalian, China.
‡Electronic address: suzuki@ims.ac.jp

[1] J. P. Heritage, T. K. Gustafson, and C. H. Lin, Phys. Rev. Lett. **34**, 1299 (1975).
[2] P. M. Felker, J. S. Baskin, and A. H. Zewail, J. Phys. Chem. **90**, 724 (1986).
[3] P. M. Felker and A. H. Zewail, J. Chem. Phys. **86**, 2460 (1987).
[4] J. S. Baskin, P. M. Felker, and A. H. Zewail, J. Chem. Phys. **86**, 2483 (1987).
[5] N. F. Scherer, L. R. Khundkar, T. S. Rose, and A. H. Zewail, J. Phys. Chem. **91**, 6478 (1987).
[6] M. Dantus, M. H. M. Janssen, and A. H. Zewail, Chem. Phys. Lett. **181**, 281 (1991).
[7] C. Riehn, A. Weichert, and B. Brutschy, Phys. Chem. Chem. Phys. **2**, 1873 (2000).
[8] A. V. Golovin, Opt. Spektrosk. I **71**, 933 (1991).
[9] P. A. Hatherly, J. Adachi, E. Shigemasa, and A. Yagishita, J. Phys. B, At. Mol. Opt. Phys. **28**, 2643 (1995).
[10] J. A. Davies, R. E. Continetti, D. W. Chandler, and C. C. Hayden, Phys. Rev. Lett. **84**, 5983 (2000).
[11] S. N. Dixit, D. L. Lynch, V. McKoy, and W. M. Huo, Phys. Rev. A **32**, 1267 (1985).
[12] H. Rudolph and V. McKoy, J. Chem. Phys. **91**, 2235 (1989).
[13] S. W. Allendorf, D. L. Leahy, D. C. Jacobs, and R. N. Zare, J. Chem. Phys. **91**, 2216 (1989).
[14] K. L. Reid, D. J. Leahy, and R. N. Zare, J. Chem. Phys. **95**, 1746 (1991).
[15] S. Kaesdorf, G. Schonhense, and U. Heinzmann, Phys. Rev. Lett. **54**, 885 (1985).
[16] J. G. Underwood and K. L. Reid, J. Chem. Phys. **113**, 1067 (2000).
[17] S. C. Althorpe and T. Seideman, J. Chem. Phys. **110**, 147 (1999).
[18] K. L. Reid, T. A. Field, M. Towrie, and P. Matousek, J. Chem. Phys. **111**, 1438 (1999).
[19] T. Suzuki, L. Wang, and H. Kohguchi, J. Chem. Phys. **111**, 4859 (1999).
[20] L. Wang, H. Kohguchi, and T. Suzuki, Faraday Discuss. **113**, 37 (1999).
[21] A. T. J. B. Eppink and D. H. Parker, Rev. Sci. Instrum. **68**, 3477 (1997).
[22] B.-Y. Chang, R. C. Hoetzlein, J. A. Mueller, J. D. Geiser, and P. L. Houston, Rev. Sci. Instrum. **69**, 1665 (1998).
[23] M. J. Cooper, P. J. Jackson, L. J. Rogers, A. J. Orr-Ewing, M. N. R. Ashfold, and B. J. Whitaker, J. Chem. Phys. **109**, 4367 (1998).
[24] N. Yonekura, C. Gebauer, H. Kohguchi, and T. Suzuki, Rev. Sci. Instrum. **70**, 3265 (1999).
[25] K. K. Innes, I. G. Ross, and W. R. Moomaw, J. Mol. Spectrosc. **132**, 492 (1988), and reference therein.
[26] K. W. Holtzclaw, L. H. Spangler, and D. W. Pratt, Chem. Phys. Lett. **161**, 347 (1989).
[27] P. M. Felker and A. H. Zewail, Chem. Phys. Lett. **128**, 221 (1986).
[28] C. N. Yang, Phys. Rev. **74**, 764 (1948).